BJP BRITISH JOURNAL OF PHARMACOLOGY

BPS BRITISH PHARMACOLOGICAL SOCIETY

British Journal of Pharmacology (2010), 160, 311–321

0007-1188/10
www.brjpharmacol.org

RESEARCH PAPER

Increased brain damage after ischaemic stroke in mice lacking the chemokine receptor CCR5

S Sorce[1], J Bonnefont[1], S Julien[1], N Marq-Lin[2], I Rodriguez[3], M Dubois-Dauphin[1#] and KH Krause[1#]

[1]*Department of Pathology and Immunology, Faculty of Medicine, University of Geneva, Geneva, Switzerland,* [2]*Department of Medical Genetics and Development, Faculty of Medicine, University of Geneva, Geneva, Switzerland, and* [3]*Department of Zoology and Animal Biology, Faculty of Sciences, University of Geneva, Geneva, Switzerland*

Background and purpose: The chemokine receptor CCR5 is well known for its function in immune cells; however, it is also expressed in the brain, where its specific role remains to be elucidated. Because genetic factors may influence the risk of developing cerebral ischaemia or affect its clinical outcome, we have analysed the role of CCR5 in experimental stroke.
Experimental approach: Permanent cerebral ischaemia was performed by occlusion of the middle cerebral artery in wild-type and CCR5-deficient mice. Locomotor behaviour, infarct size and histochemical alterations were analysed at different time points after occlusion.
Key results: The cerebral vasculature was comparable in wild-type and CCR5-deficient mice. However, the size of the infarct and the motor deficits after occlusion were markedly increased in CCR5-deficient mice as compared with wild type. No differences between wild-type and CCR5-deficient mice were elicited by occlusion with respect to the morphology and abundance of astrocytes and microglia. Seven days after occlusion the majority of CCR5-deficient mice displayed neutrophil invasion in the infarct region, which was not observed in wild type. As compared with wild type, the infarct regions of CCR5-deficient mice were characterized by increased neuronal death.
Conclusions and implications: Lack of CCR5 increased the severity of brain injury following occlusion of the middle cerebral artery. This is of particular interest with respect to the relatively frequent occurrence of CCR5 deficiency in the human population (1–2% of the Caucasian population) and the advent of CCR5 inhibitors as novel drugs.
British Journal of Pharmacology (2010) **160,** 311–321; doi:10.1111/j.1476-5381.2010.00697.x

Keywords: brain; chemokine receptor; CCR5; genetics; cerebral ischaemia; stroke; neuronal death

Abbreviations: DNase, deoxyribonuclease; GFAP, glial fibrillary acidic protein; IBA-1, ionized calcium binding adapter molecule-1; MCA, middle cerebral artery; MCAo, MCA occlusion; MIP, macrophage inflammatory protein; MPO, myeloperoxidase; NeuN, neuronal nuclei; RANTES, regulated on activation, T cell expressed and secreted; TdT, terminal deoxyribonucleotidyl transferase; TUNEL, TdT-mediated dUTP nick end labelling

Introduction

Chemokines are small proteins that play a key role in the regulation of leukocyte maturation and trafficking (Rossi and Zlotnik, 2000). However, chemokines and their corresponding receptors are also expressed in the CNS and regulate glial and neuronal cell functions (Cartier *et al.*, 2005; Rostene *et al.*, 2007). Because of its involvement in HIV entry into cells (Alkhatib *et al.*, 1996), the chemokine receptor CCR5 (nomenclature follows Alexander *et al.*, 2009) has become one of the most studied chemokine receptors and represents a new pharmacological target for HIV therapy. The CCR5 G-protein-coupled receptor is stimulated by three β-chemokines: CCL3/macrophage inflammatory protein-1α (MIP-1α), CCL4/MIP-1β and CCL5/regulated on activation, T cell expressed and secreted (Oppermann, 2004). Although constitutive CCR5 expression has been detected in astrocytes, microglia and neurons (Rottman *et al.*, 1997; Westmoreland *et al.*, 2002; Torres-Munoz *et al.*, 2004), its role in healthy brain is still poorly understood. On the other hand, it has been reported that CCR5 is up-regulated after neurological insults (Galasso *et al.*, 1998; Simpson *et al.*, 2000) and might be involved in pathogenesis, in particular with respect to HIV-associated dementia (Kaul and Lipton, 2006).

Correspondence: KH Krause, Department of Pathology and Immunology, Faculty of Medicine, University of Geneva, Rue Michel-Servet 1, 1211 Geneva-4, Switzerland. E-mail: Karl-Heinz.Krause@unige.ch
#These authors have equally contributed.
Received 6 July 2009; revised 7 October 2009; accepted 2 December 2009

Brain damage after stroke is the result of complex biochemical and cellular mechanisms. Indeed, following ischaemia, hypoxia-dependent necrosis occurs in the infarct core with irreversible consequences. Subsequently, several molecular pathways are activated and can be either protective or detrimental to the neighbouring regions that are functionally impaired, but potentially salvageable (Mehta *et al*., 2007). The evolution of such mechanisms determines the final extent of the infarct. The genetic background may also influence the clinical outcome of strokes. Indeed, genetic factors may either increase the risk of developing a stroke (Dichgans, 2007) or modulate the outcome in response to a given ischaemic lesion (Mallolas *et al*., 2006). There is evidence for increased CCR5 expression following focal cerebral ischaemia (Spleiss *et al*., 1998; Cowell *et al*., 2002; Kremlev *et al*., 2007). So far, it is not clear whether this up-regulation has a functional importance; however, this appears to be an important clinical question, as about 1–2% of the Caucasian population is homozygous for a 32 base-pair deletion in the coding sequence of the *CCR5* gene (Martinson *et al*., 1997; Libert *et al*., 1998). This deletion impairs CCR5 conformation and leads to its degradation (Liu *et al*., 1996). The absence of CCR5 is detrimental in certain types of infection (Barr *et al*., 2005; Hardison *et al*., 2006; Khan *et al*., 2006) and can lead to severe complications in the CNS (Huffnagle *et al*., 1999; Glass *et al*., 2005; 2006; Thapa *et al*., 2007). In addition to the 32 base-pair deletion, numerous polymorphisms, influencing the activity of the CCR5 receptor, have been identified (Blanpain *et al*., 2000). Also, the recent introduction of CCR5 antagonists for the treatment of HIV (Emmelkamp and Rockstroh, 2007) requires an improved understanding of the potential negative effects of the lack of functional CCR5 (Stephenson, 2007).

In order to investigate whether CCR5 can influence the extent of brain damage induced by stroke, we analysed the effects of permanent middle cerebral artery occlusion (MCAo) in wild-type and CCR5 knockout mice. Our results show an enhancement of the post-ischaemic injury in CCR5-deficient mice and suggest a neuroprotective role of CCR5.

Methods

Mice

All animal care and experimental procedures were approved by the ethical committee of the University of Geneva and the Cantonal Veterinary Office. The CCR5-deficient mice in the C57BL/6 background (Kuziel *et al*., 2003) were kindly provided by Professor SS Ahuja (University of Texas at Austin, USA). Food and water were supplied *ad libitum* in a quiet room at 25°C with a 12 h light/dark cycle. Male mice of 8–10 weeks of age were used for MCAo.

MCA_o

Surgical operations were performed as previously described (De Bilbao *et al*., 2000). Briefly, the right temporo-parietal region of the head was shaved and a 2 mm incision was made vertically between the orbit and the ear. Under an operating microscope, a small burr hole (1 mm^2) was made with a high-speed micro-drill to expose temporal vessels. After identification, the MCA was occluded by electrocoagulation using a small cauterizer without damaging the brain surface. The duration of the surgery did not exceed 15 min. Arterial blood pressure and blood parameters (pH, glucose, O_2 and CO_2 pressure) were analysed in randomly selected mice ($n = 6$ per group) before and after the MCAo surgery.

Wild-type and CCR5-deficient mice were killed at 2 and 7 days after MCAo and processed for histological analysis. After perfusion with a solution of 4% paraformaldehyde in phosphate-buffered saline (PBS) (pH 7.35), brains were removed, paraffin-embedded and cut in 10 µm thick sections.

Infarct analysis

Quantification of the infarct area was performed on cresyl violet-stained sections throughout the rostro-caudal extent of the lesion. For each brain slice, the infarcted area and the area of the whole section (total brain area in the right and left hemispheres) were measured using the Metamorph software (Molecular Devices, Sunnyvale, CA, USA). Infarct area was calculated as a percentage of the whole brain section analysed. Rostro-caudal extension of the infarct was measured from rostral pole, at the lateral septum level, to caudal pole, at the posterior thalamus/mesencephal level, corresponding to the brain territory covered by the MCA. Slides were coded so that the analysis was made blindly.

Grip test

Motor deficits were assessed by a grip test as previously described (Haddad *et al*., 2006) from 1 to 7 days after MCAo. Mice were picked up by the tail and placed on a taut string 60 cm long suspended 40 cm above a table. Grip score was measured as the length of time that mice remained on the string in some manner (using one or more paws, tail, tail plus paws) for a maximum of 30 s. Each experiment was conducted randomly and blindly in order to avoid uncontrolled influences.

Analyses of cerebral vasculature

Mice were anaesthetized and perfused transcardially with carbon black to visualize cerebral vasculature. After 10 min, animals were decapitated and heads stored in 4% paraformaldehyde for 48 h at 4°C. Brains were carefully removed and photographs were taken of the dorsal brain surfaces. Cerebral vasculature analysis was performed as previously described (Maeda *et al*., 1998). The distance from the inter-hemispheric fissure and the anterior cerebral artery and MCA anastomoses was measured at coronal planes 2, 5 and 7 mm from the frontal pole.

Semi-quantitative end-point PCR

Total RNA was isolated from homogenized tissues using RNeasy mini kit (Qiagen, Hombrechtikon, Switzerland) according to the manufacturer's instructions. Residual genomic DNA was removed using RNase-free DNase (deoxyribonuclease) set (Qiagen). Total RNA (1 µg) was reverse transcribed using the superscript II kit according to the

Table 1 Oligonucleotide probes and conditions used for semi-quantitative end-point RT-PCR

Gene	*Primer sequences*	*Product size*	*Tm*	*# cycles*
Ccr5	F: GCT GCC TAA ACC CTG TCA TC R: GTT CTC CTG TGG ATC GGG TA	199	60	32
Ccl3	F: ATG AAG GTC TCC ACC ACT GC R: CCC AGG TCT CTT TGG AGT CA	279	60	32
Ccl4	F: GCC CTC TCT CTC CTC TTG CT R: GTC TGC CTC TTT TGG TCA GG	196	60	32
Ccl5	F: CCC TCA CCA TCA TCC TCA CT R: CCT TCG AGT GAC AAA CAC GA	185	60	32
L32	F: GTG AAG CCC AAG ATC GTC AA R: TTG GTG ACT CTG ATG GCC AG	349	58	*26*

manufacturer's instructions (Invitrogen, Basel, Switzerland). Semi-quantitative end-point PCR was performed by determining the suitable number of PCR cycles giving linear cDNA amplification of each gene of interest using Taq DNA polymerase (Qiagen). Amplification of the housekeeping gene encoding the L32 ribosomal protein was used as control. The list of the primers used is given in Table 1. PCR bands were scanned, and optical densities were analysed by ImageJ software (http://rsb.info.nih.gov/ij/).

Immunohistochemistry

Brain sections were deparaffinized through graded alcohols, subjected to heat-induced epitope retrieval for 15 min in 0.01 M citrate buffer, pH 6.0, and incubated overnight at 4°C with primary antibodies diluted in PBS/0.3% Triton-X100 buffer at the following concentrations: myeloperoxidase 1:500 (MPO; Dako, Baar, Switzerland), glial fibrillary acidic protein 1:2000 (GFAP, Millipore, Billerica, MA, USA), ionized calcium binding adapter molecule-1 1:500 (IBA-1, Dako) and neuronal nuclei 1:1000 (NeuN, Millipore). Sections were then incubated for 1 h at room temperature with a biotinylated secondary antibody (Vector laboratories, Peterborough, UK). After several washes in PBS, sections were incubated with the ABC complex solution (Vector laboratories). Tissue-bound peroxidase was visualized using 3,3′-diaminobenzidine (DAB, Sigma-Aldrich, St. Louis, MO, USA) and H_2O_2. Counterstaining with cresyl violet was performed to visualize cell nuclei. Negative controls in the absence of the primary antibodies were performed for each experiment (data not shown). The surface occupied by GFAP, IBA-1 or MPO stained cells was measured at different coronal levels, using the Metamorph software (Molecular Devices): regions of interest (cortical infarct, neighbouring cortex and striatum, where cell density was increased for GFAP and IBA-1 immunoreactivity, and infarct core for MPO immunoreactivity) were designed according to stereotaxic coordinates (Franklin and Paxinos, 1997) and the pixels stained above threshold determined. Values are expressed as the ratio between the stained regions respect to the total area measured. The number of NeuN-positive cells was calculated as previously described (Schroeter *et al*., 2006) and using the Metamorph software (Molecular Devices): the number of neuronal cells (identified by NeuN staining) in the infarct core was automatically counted on digitally stored images and defined as the number of NeuN-stained cells for tissue area (neuronal density ipsi). For each brain slide, the neuronal density was similarly calculated in the corresponding brain area of the contralateral hemisphere (neuronal density contra), defined following stereotaxic coordinates (Franklin and Paxinos, 1997). Finally, the number of neurons in the infarct core was calculated as the ratio between neuronal density ipsi and neuronal density contra, and expressed as a percentage. In addition, a double labelling for terminal deoxyribonucleotidyl transferase (TdT)-mediated dUTP nick end labelling (TUNEL) staining and NeuN immunoreactivity was performed (described below). Neuronal cells in the infarct core identified by both markers were counted off-line on digitally stored high-power images. All the quantifications were made blindly.

In situ hybridization

In order to combine fluorescent *in situ* hybridization with fluorescent immunohistochemical detection, brain sections of mice after permanent MCAo were subjected to deparaffinization and heat-mediated epitope retrieval as described above, and hybridized according to the protocol from Roppolo *et al*. (2007). Digoxigenin-labelled *Ccr5* RNA probe was obtained from Eurexpress Consortium (http://www.eurexpress.org) and prepared using the DIG RNA labelling kit (Roche, Basel, Switzerland) following the manufacturer's instructions. After detection of the *Ccr5* mRNA Fast red fluorescent signal, sections were incubated overnight at 4°C with primary antibodies and then for 1 h at room temperature with secondary antibody AlexaFluor 488 (Molecular Probes, Basel, Switzerland). Cell nuclei were stained with DAPI. Imaging was performed on a LSM 510 Meta confocal laser scanner mounted on an Axio Imager Z1 microscope (Carl Zeiss, Feldbach, Switzerland). We used brain sections of CCR5-deficient mice also subjected to permanent MCAo as negative control.

TUNEL

TUNEL staining was done as previously described (De Bilbao *et al*., 2000) using recombinant terminal transferase, following the manufacturer's instructions (Roche). Single staining: TUNEL signal was detected by using a horseradish peroxidase HRP–ABC complex solution (1:100, Vector laboratories) visualized with DAB and H_2O_2. Double staining with NeuN: sections were deparaffinized, subjected to heat-induced epitope retrieval and incubated with NeuN antibody (as described above). After NeuN detection with an Alexa 555-labelled secondary antibody, sections were processed for TUNEL staining. In this case, TUNEL signal was detected with Alexa 488-labelled secondary antibody for streptavidin. Cell nuclei were stained with DAPI. Negative controls of TUNEL staining were performed by omitting TdT. The number of apoptotic/necrotic neurons was determined by counting the NeuN/TUNEL double-stained cells in the infarct region.

Statistical analysis

Results are expressed as means ± standard error of the mean. Statistical analyses were performed using the appropriate test

as indicated in the figure legends (Student's *t*-test, one-way or two-way analysis of variance followed by *post hoc* Tukey's test). For all tests, a *P*-value < 0.05 was taken as statistically significant.

Results

Enhanced stroke-related brain damage in CCR5-deficient mice

In order to assess the role of CCR5 in cerebral stroke outcome, we compared brain lesions 2 and 7 days after permanent MCAo in wild-type and CCR5-deficient mice. Two days after ischaemia, the rostro-caudal extension of the infarct was similar in CCR5-deficient mice, as compared with wild type (Figure 1F), while the area of the infarct core was significantly larger, mainly on its latero-medial extension from cortex to sub-cortical structures (39.7% more than wild type; Figure 1A vs. B and E). Seven days after MCAo, in both wild-type and CCR5-deficient mice the area of the infarct core was reduced (Figure 1E), in agreement with previous reports (De Bilbao *et al.*, 2000; Schroeter *et al.*, 2006). However, the length of the infarct remained unchanged in wild-type mice, extending from the level of anterior lateral septum [bregma 1.54 mm; (Franklin and Paxinos, 1997)] to the level of the posterior thalamus–anterior mesencephalon junction and ventral hippocampus [bregma –2.54 mm; (Franklin and Paxinos, 1997)]. The infarct core encompassed mainly the sensory cortex and was generally limited by the external capsule with few extensions into the striatum, but none into the thalamus (Figure 1C). Conversely, in CCR5-deficient mice, the extent of cortical brain damage was markedly increased along the anteroposterior axis, reaching up to the level of the superior colliculus, in the mesencephalon. As compared with wild type, the infarct was also more developed: (i) on the dorsoventral axis, in the cortex, reaching the motor cortex; and (ii) on the lateromedial axis, beyond the external capsule into the striatum, namely in the caudate–putamen complex (Figure 1D). Quantification of the size of the lesions indicated that CCR5 deficiency caused a significantly increased infarct core (88.6% more than wild type; Figure 1E) and rostro-caudal extension (39.7% more than wild type; Figure 1F), namely by reaching part of the auditory and visual cortex at the level of the superior colliculus [bregma –3.64 mm; (Franklin and Paxinos, 1997)]. Therefore, the presence of functional CCR5 appeared to limit cerebral injury after MCAo.

Absence of CCR5 does not influence cerebral vasculature or physiological parameters

Several studies have demonstrated that individual and strain-related differences in the cerebrovascular architecture influence MCAo-induced brain lesion size (Connolly *et al.*, 1996; Maeda *et al.*, 1998). Hence, we performed carbon black labelling of cerebral vasculature in wild-type and CCR5-deficient mice. We measured the distances between the inter-hemispheric fissure and the anterior cerebral artery and MCA anastomoses. As shown in Figure 2A, we did not observe any difference in the superficial cerebrovascular architecture that could account for the different infarct sizes between wild-type and CCR5-deficient mice. Alterations of systemic physiological parameters can also modify outcome after cerebral stroke. We therefore analysed these parameters before and after MCAo. We did not observe any significant difference in arte-

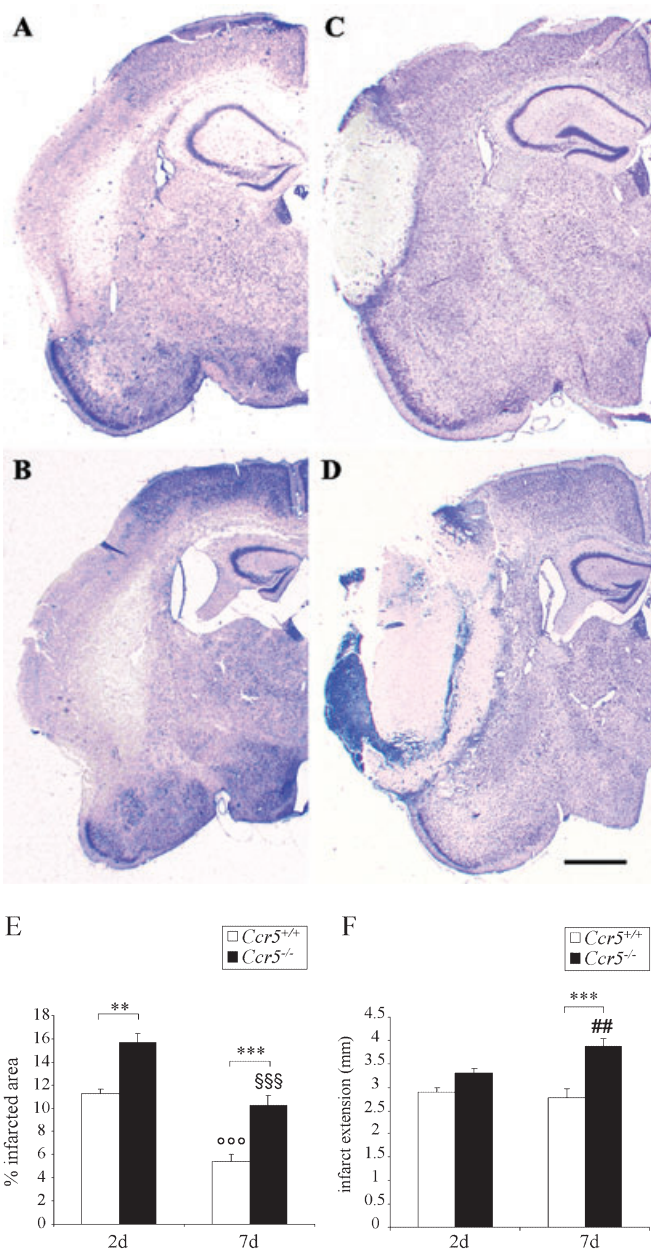

Figure 1 Increased infarct size in CCR5-deficient (*Ccr5*$^{-/-}$) mice. Male mice were subjected to permanent middle cerebral artery occlusion (MCAo) and killed at 2 and 7 days after stroke. (A–D) Representative brain sections (10 μm) stained with cresyl violet of wild-type (*Ccr5*$^{+/+}$; A,C) and CCR5-deficient (B,D) mice brains 2 days (A,B) and 7 days (C,D) after stroke. Scale bar: 1 mm. (E) Infarcted areas were calculated as a percentage of the whole brain region examined. $^{**}P < 0.01$ and $^{***}P < 0.001$ *Ccr5*$^{-/-}$ versus *Ccr5*$^{+/+}$ mice 2 and 7 days after MCAo, $^{°°°}P < 0.001$ *Ccr5*$^{+/+}$ mice 2 versus 7 days, $^{§§§}P < 0.001$ *Ccr5*$^{-/-}$ mice 2 versus 7 days using two-way ANOVA followed by Tukey's *post hoc* test. (F) The rostro-caudal extension was measured between the rostral pole, at the lateral septum level, and the caudal pole, at the posterior thalamus/mesencephal level. $^{***}P < 0.001$ *Ccr5*$^{-/-}$ versus *Ccr5*$^{+/+}$ mice 7 days after MCAo, $^{##}P < 0.01$ *Ccr5*$^{-/-}$ 7 versus 2 days using two-way ANOVA followed by Tukey's *post hoc* test ($n = 5–8$).

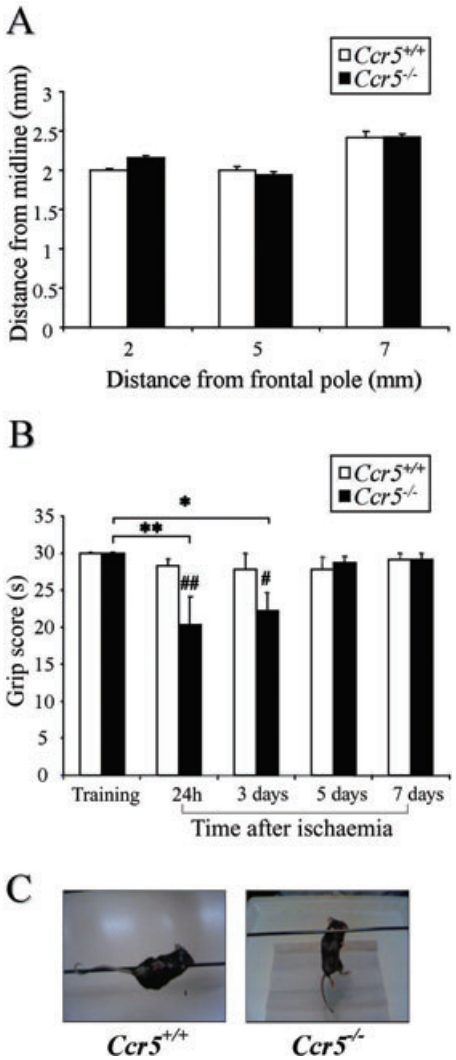

Figure 2 Cerebral vasculature and stroke-induced motor deficits in wild-type (*Ccr5*$^{+/+}$) and CCR5-deficient (*Ccr5*$^{-/-}$) mice. (A) Cerebrovascular architecture in wild-type and CCR5-deficient mice was compared by measuring the distance from the inter-hemispheric fissure to the anastomotic line between the middle cerebral artery and the anterior cerebral artery in carbon black-perfused brains. Data are shown as mean ± standard error, $n = 3$. (B,C) Motor deficits were evaluated by performing a grip test before and after middle cerebral artery occlusion (MCAo), at different time points before sacrifice. (B) Grip score before (training) and at different time points following MCAo. *$P < 0.05$, **$P < 0.01$ *Ccr5*$^{-/-}$ mice training versus 3 days and 24 h after MCAo; $^{\#}P < 0.05$ *Ccr5*$^{+/+}$ versus *Ccr5*$^{-/-}$ mice 3 days after MCAo; $^{\#\#}P < 0.01$ *Ccr5*$^{+/+}$ versus *Ccr5*$^{-/-}$ mice 24 h after MCAo using two-way ANOVA followed by Tukey's *post hoc* test ($n = 6$). (C) Representative images of motor behaviour displayed by *Ccr5*$^{+/+}$ and *Ccr5*$^{-/-}$ mice during the grip test 7 days after MCAo.

rial blood pressure and blood parameters (pH, glucose, O_2 and CO_2 pressure) before and after experimental stroke between wild-type and CCR5-deficient mice (Table 2).

Increased motor deficits in CCR5-deficient mice

In order to examine post-ischaemic neurological deficits, we performed a grip test, which allows the detection of motor function impairment. In this behavioural test, wild-type mice did not exhibit significant motor deficit following cerebral ischaemia (Figure 2B and Video S1). In contrast, the motor performance of CCR5-deficient mice was significantly diminished at 24 h and 3 days after MCAo (Figure 2B and Video S1). At later time points, CCR5-deficient mice showed spontaneous functional recovery and were able to grip until they reached the threshold time. Spontaneous functional recovery in rodents has been previously described (Hunter *et al*., 2000; Zausinger *et al*., 2000). However, the pattern of behaviour during the grip test remained distinct. While wild-type mice gripped with four paws and the tail, CCR5-deficient mice gripped with only one or two paws, barely finding a position of equilibrium on the string (Figure 2C).

Thus, increased post-ischaemic lesions in CCR5-deficient mice led to impaired motor functions.

Expression of Ccr5 after MCAo

We analysed the transcriptional expression of *Ccr5* in the brain of wild-type mice following permanent MCAo. Twenty-four hours and 7 days after stroke, the mRNA levels of *Ccr5* and its ligands *Ccl3*, *Ccl4* and *Ccl5* were increased in the hemisphere ipsilateral to the lesion as compared with the contralateral hemisphere (Figure 3A, G). The concomitant expression of CCR5 ligands suggested that CCR5 receptor may also be activated. We also performed *in situ* hybridization experiments in order to define in which cells *Ccr5* was expressed. In wild-type mice the *Ccr5* mRNA signal was punctiform (Figure 3B), a distribution observed for other genes (Daberkow *et al*., 2007; Sonomura *et al*., 2007). The *Ccr5* mRNA probe did not yield any signal in CCR5-deficient mouse brain sections (Figure 3C). In agreement with previous reports (Rottman *et al*., 1997; Westmoreland *et al*., 2002; Torres-Munoz *et al*., 2004), we observed that *Ccr5* was present in neurons, astrocytes and microglia (Figure 3D–F).

Astrocyte and microglia response after MCAo in wild-type and CCR5-deficient mice

Given that inflammatory processes may contribute to differences in the extent of post-ischaemic lesions (Wang *et al*., 2007) and that *Ccr5* was expressed in astrocytes and microglia (Figure 3E–F), we compared the inflammatory cell response to ischaemia in wild-type and CCR5-deficient mice. Astrocytes were detected with a GFAP antibody and activated microglia/macrophages with an IBA-1 antibody. Two days after MCAo, only relatively low amounts of astrocytes and activated microglia were detected. Conversely, 7 days after permanent MCAo, GFAP- and IBA-1-immunoreactive cells were accumulated in structures anatomically connected with the infarct (Figure 4A–L), such as the surrounding cortex, the striatum, the ipsilateral thalamus nuclei (posterior and ventro-posterior), the corpus callosum, as well as the contralateral cortex and thalamus. Considering the respective infarct area, there were no differences in the amount of GFAP- or IBA-1-immunoreactive cells between wild-type and CCR5-deficient mice (Figure 4Q–V). Also, both astrocytes and microglia did not show altered morphology in CCR5-deficient mice (Figure 4M–P). Thus, absence of CCR5 does not influence glia recruitment or morphological appearance.

Table 2 Physiological parameters before and after permanent middle cerebral artery occlusion (MCAo) in wild-type (*Ccr5*$^{+/+}$) and CCR5-deficient (*Ccr5*$^{-/-}$) mice

	Before MCAo		*After MCAo*	
	Ccr5$^{+/+}$	*Ccr5*$^{-/-}$	*Ccr5*$^{+/+}$	*Ccr5*$^{-/-}$
Glucose (mg·mL^{-1})	1.73 ± 0.09	1.78 ± 0.09	1.64 ± 0.09	1.51 ± 0.09
pH	7.39 ± 0.01	7.35 ± 0.02	7.39 ± 0.02	7.35 ± 0.02
pCO_2 (kPa)	5.14 ± 0.19	5.18 ± 0.09	5.26 ± 0.17	5.56 ± 0.08
pO_2 (kPa)	9.59 ± 0.43	9.94 ± 0.22	9.02 ± 0.44	9.27 ± 0.31
Arterial blood pressure (mmHg)	105 ± 2	101 ± 2	102 ± 4	100 ± 3

Blood parameters (glucose, pH, CO_2 and O_2 pressure) and arterial blood pressure were analysed in wild-type (*Ccr5*$^{+/+}$) and CCR5-deficient (*Ccr5*$^{-/-}$) mice before and after permanent MCAo. No statistical significant differences were found using two-way ANOVA ($n = 6$).

Neutrophil recruitment after stroke in wild-type and CCR5-deficient mice

We analysed neutrophil recruitment in ischaemic lesions by staining with an antibody against MPO. Neutrophils were barely detected in wild-type mice, at both 2 and 7 days after stroke (Figure 5A,C). In contrast, CCR5-deficient mice displayed a massive invasion of the infarct core by neutrophils 7 days after ischaemia (Figure 5D,F). However, no such invasion was observed at the earlier time point (2 days, Figure 5B, E), suggesting that neutrophil accumulation at injured regions is a late event.

Increased neuronal death in CCR5-deficient mice

The increased infarct size in CCR5-deficient mice might be associated with a decreased neuronal survival. We therefore analysed the neurons in the infarct core that were still immunoreactive for NeuN antibody, as well as the signs of cell death using TUNEL labelling. By counting NeuN-immunoreactive cells in the infarct region, we observed a significant decrease in the number of neurons in CCR5-deficient mice (Figure 6G). In support of this observation, the number of TUNEL-positive cells was markedly increased in CCR5-deficient mice as compared with wild type (Figure 6A vs. B and H). Double staining with NeuN antibody and TUNEL labelling suggested that the majority of dying cells in CCR5-deficient infarcts were neurons (Figure 6C–F). Thus, the greater brain damage in CCR5-deficient mice was associated with increased neuronal death in the infarct region.

Discussion and conclusions

In this study, we show that CCR5 deficiency in mice exacerbates the severity of cerebral infarction after MCAo. In ischaemic brains, CCR5 was expressed in neurons, astrocytes and microglia. The infarct region of CCR5-deficient mice was characterized by strikingly increased neuronal injury, without detectable changes in astrocytes and microglia. Thus, CCR5 expression is neuroprotective in this mouse stroke model.

The fact that CCR5 contributes to protective mechanisms in stroke points towards a unique role of this chemokine receptor. Indeed, the interaction of chemokines with their receptors promotes leukocyte trafficking and inflammation and is therefore expected to aggravate cerebral infarction. In support of this concept, mice deficient for CCR2, CCL2 (=CCR2 ligand), or CX3CL1 (=CX_3CR1 ligand) showed decreased infarct size after ischaemic stroke (Hughes *et al*., 2002; Soriano *et al*., 2002; Dimitrijevic *et al*., 2007). Similarly, several chemokine inhibitors or antagonists of chemokine receptors reduced brain damage after stroke: (i) TAK779, a CCR2 antagonist in mice (Takami *et al*., 2002; Saita *et al*., 2007); (ii) NR58-3.14.3 and vMIP-2, broad-spectrum antagonists of chemokine receptors (Beech *et al*., 2001; Takami *et al*., 2001); (iii) repertaxin, a CXCL8 inhibitor (Garau *et al*., 2005); and (iv) DF2156A, a dual inhibitor of CXCR1 and CXCR2 (Garau *et al*., 2006). However, here we report that CCR5 deficiency aggravates brain damage and behavioural outcome after cerebral stroke.

Such a protective role of CCR5 could not have been predicted from inflammatory pathologies outside the CNS. For example, there is evidence for a detrimental role of CCR5 in experimental atherosclerosis (Braunersreuther *et al*., 2007), in development of human cardiovascular disease (Afzal *et al*., 2008), and in experimental pulmonary emphysema (Ma *et al*., 2005). In contrast, there are indications for a protective effect of CCR5 in the CNS. Indeed, CCR5-deficient mice infected with *Cryptococcus neoformans*, herpes simplex virus type 2 or West Nile virus, displayed increased severity of CNS damage (Huffnagle *et al*., 1999; Glass *et al*., 2005; Thapa *et al*., 2007). In these cases, the protection by CCR5 was attributed to its capacity to increase host-defence through CCR5-dependent regulation of leukocyte trafficking. The fact that such a protective role is also found in a non-infectious condition, such as stroke, might hint towards a more global role of CCR5 in neuroprotection. Several lines of argument support this concept. Thus, stimulation of endogenous CCR5 by its natural ligands triggered neuroprotective mechanisms and prevented apoptosis in response to the HIV envelope protein gp120 (Meucci *et al*., 1998; Kaul and Lipton, 1999; Catani *et al*., 2000; Kaul *et al*., 2007). Further, the CCR5 ligands CCL3 and CCL4 prevent excitotoxicity induced by NMDA (Bruno *et al*., 2000) and nerve injury-induced motor neuron death was accelerated in CCR5-deficient mice (Gamo *et al*., 2008).

The mechanism underlying the protective effect of CCR5 after stroke could be due to its capacity to regulate inflammatory response. Glia abundance and morphology is not altered

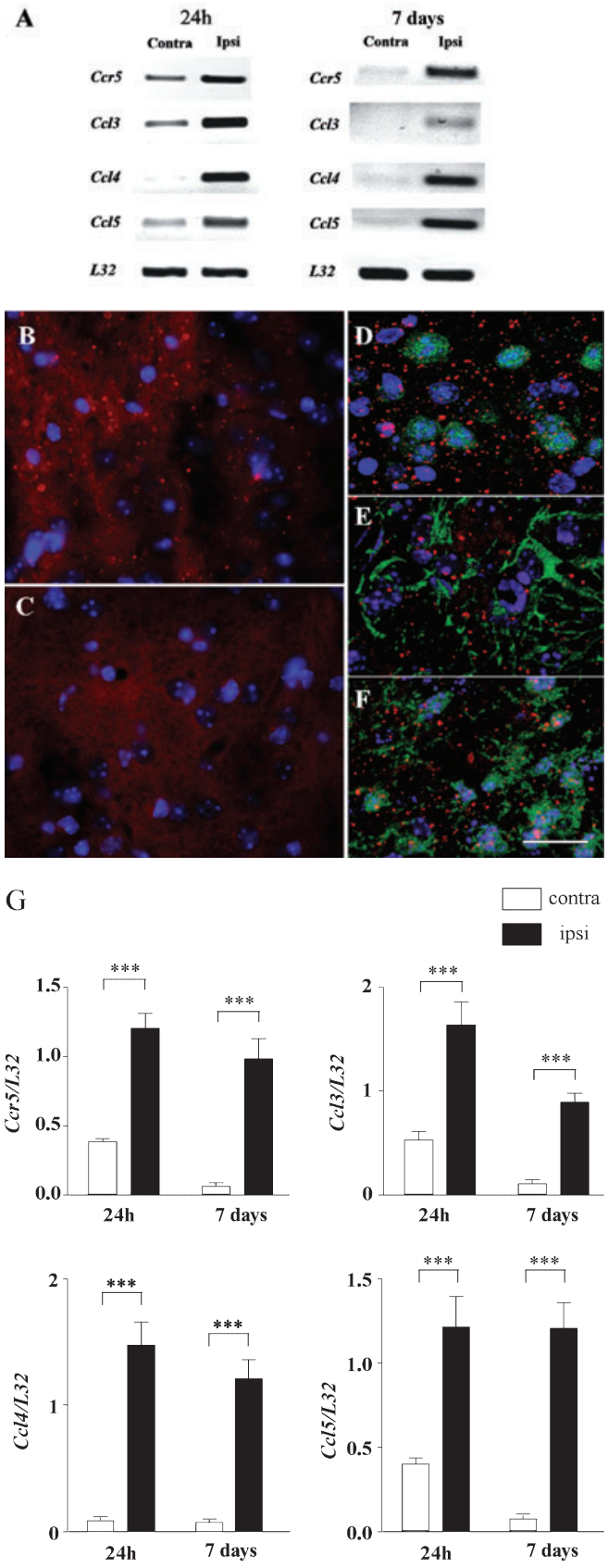

Figure 3 Expression of *Ccr5* and its ligands (*Ccl3*, *Ccl4* and *Ccl5*) after permanent middle cerebral artery occlusion (MCAo). Wild-type mice ($Ccr5^{+/+}$) were subjected to experimental stroke through permanent MCAo. (A) The mRNA extracted from contralateral and ipsilateral parts of the brain 24 h and 7 days after stroke was analysed by RT-PCR. The ribosomal *L32* house keeping gene was used as control. Similar results were obtained from four animals. (B,C) *In situ* hybridization was performed on $Ccr5^{+/+}$ and $Ccr5^{-/-}$ brain sections after permanent MCAo. Representative images of $Ccr5^{+/+}$ (B) and $Ccr5^{-/-}$ (C) brain sections (infarct border) showing *Ccr5* mRNA signal (red dots) and DAPI staining (blue). Scale bar: 25 μm. (D–F) Representative confocal images of the infarct border showing neurons (D), astrocytes (E) and microglia (F) stained, respectively, with neuronal nuclei, glial fibrillary acidic protein and ionized calcium binding adapter molecule-1 antibodies (green), *Ccr5* probe (red dots) and DAPI (blue). Scale bar: 25 μm. (G) Semi-quantitative analyses obtained through densitometric scanning of *Ccr5*, *Ccl3*, *Ccl4*, *Ccl5* RT-PCR products, normalized with respect to the ribosomal protein L32. $***P < 0.001$ using two-way ANOVA followed by Tukey's *post hoc* test ($n = 4$).

in CCR5-deficient mice after stroke (this study), hippocampal damage (Babcock *et al.*, 2003) or nerve injury-induced motoneuron death (Gamo *et al.*, 2008). Nevertheless, the last study reported evidence for a functional difference of CCR5-deficient microglia, which, *in vitro*, released increased amounts of potentially neurotoxic cytokines after exposure to LPS (Gamo *et al.*, 2008). Thus, it is possible that CCR5 limits microglia activation and neuroinflammation, thereby decreasing brain damage. This might also explain the important neutrophil invasion in CCR5-deficient brains observed at late time points in our study. Theoretically, CCR5 could be also involved in inflammatory monocyte migration into the brain after ischaemic damage (Getts *et al.*, 2008); however, the unchanged number of IBA-1-positive cells makes this possibility less likely. As CCR5 is also expressed in neurons, the possibility that it might directly regulate neuronal survival should also be considered. Indeed, there is an emerging consensus that chemokine receptors are expressed in neurons, where they modulate various neuronal functions, including neurotransmission, neuronal migration and neuronal survival (Rostene *et al.*, 2007).

An important issue raised by the protective role of CCR5 in experimental cerebral ischaemia is its potential clinical relevance for cerebrovascular pathologies in humans, from stroke to vascular dementia. In other types of pathologies, there is a good correlation between mice and humans with respect to the impact of CCR5 deficiency. This is true for the decreased peripheral cardiovascular risk (see above), but also for the increased severity of infection with West Nile virus (Glass *et al.*, 2005; 2006; Lim *et al.*, 2008). Thus, is CCR5 deficiency, found in 1–2% of the Caucasian population, a risk factor for the severity of stroke in humans? And if yes, what would be the clinical presentation? Indeed, CCR5 deficiency could lead to an increased number of mild strokes (transient ischaemic attacks presenting as stroke), or to an increased severity of stroke. This question is also interesting in the context of HIV, where the CCR5 antagonist maraviroc has been recently introduced as a treatment, which prevents HIV from entering CD4 cells *via* the CCR5 co-receptor (Emmelkamp and Rockstroh, 2007; Sayana and Khanlou, 2009). As HIV-infected individuals have an increased risk of

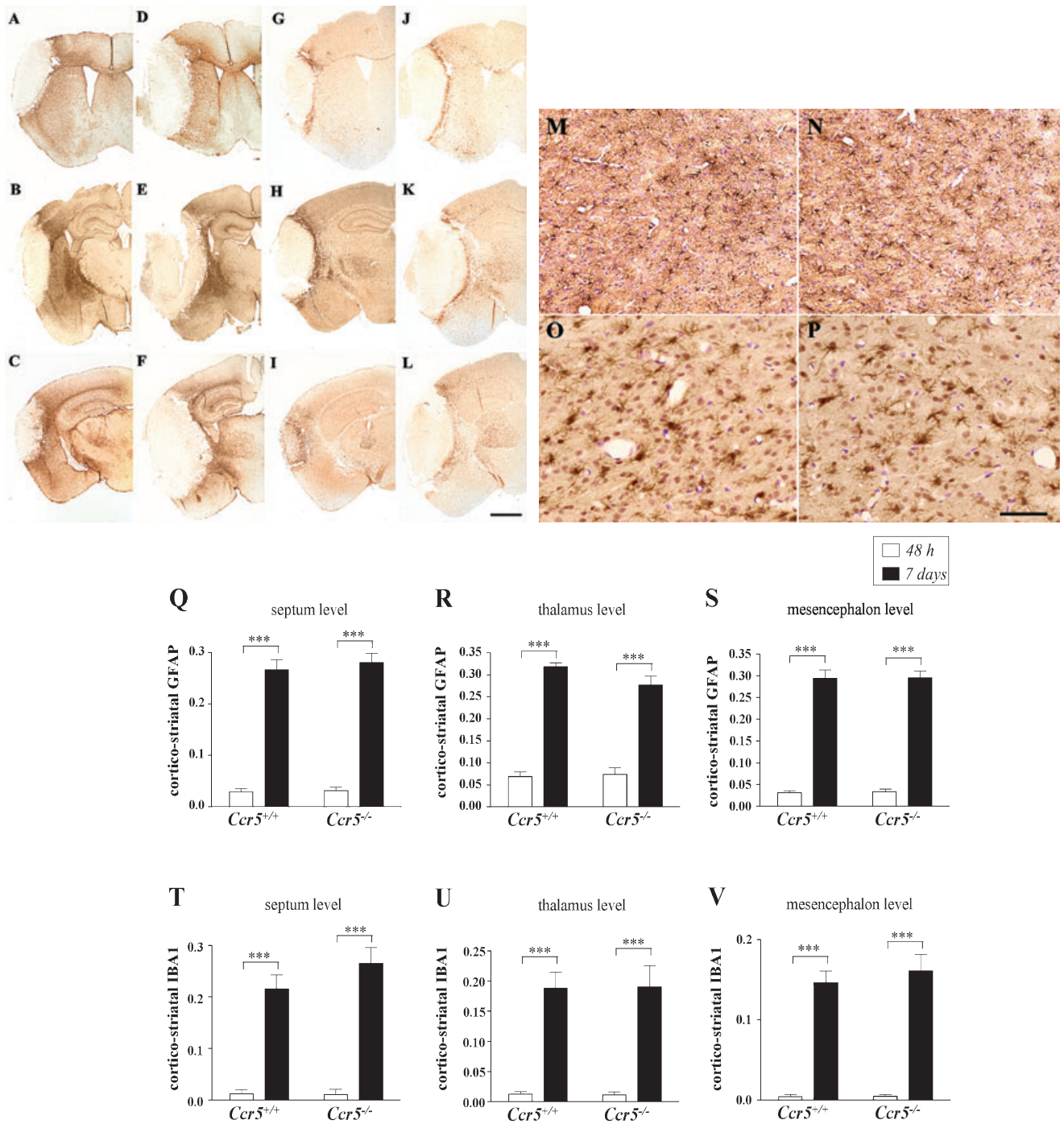

Figure 4 Astrocyte and microglia response after stroke in wild-type (*Ccr5*$^{+/+}$) and CCR5-deficient (*Ccr5*$^{-/-}$) mice. Astrocytes and microglia/macrophages were detected by immunohistochemistry with glial fibrillary acidic protein (GFAP) or ionized calcium binding adapter molecule-1 (IBA-1) antibodies, respectively, in *Ccr5*$^{+/+}$ and *Ccr5*$^{-/-}$ mouse brains 7 days after middle cerebral artery occlusion (MCAo). ($n = 8$). Representative images of (A–F) GFAP or (G–L) IBA-1 staining at different coronal levels of *Ccr5*$^{+/+}$ (A–C and G–I) and *Ccr5*$^{-/-}$ (D–F and J–L) brain sections. Scale bar: 1 mm. (M–P). High-power images showing astrocytes (M,N) and microglia (O,P) in brains of *Ccr5*$^{+/+}$ (M,O) and *Ccr5*$^{-/-}$ (N,P) mice 7 days after MCAo. Scale bar: for (M, N) 90 μm, for (O, P) 45 μm. (Q–V) Quantification of GFAP (Q–S) and IBA-1 (T–V) staining: the surface occupied by GFAP- or IBA-1-immunoreactive cells (*y*-axis) was quantified as described in the *Method* section in brain sections of *Ccr5*$^{+/+}$ and *Ccr5*$^{-/-}$ mice 2 and 7 days after MCAo. ***$P < 0.001$ using two-way ANOVA followed by Tukey's *post hoc* test. No significant differences were detected between *Ccr5*$^{+/+}$ and *Ccr5*$^{-/-}$ mice ($n = 4$–8).

developing cerebrovascular disease (Cole *et al.*, 2004; Tipping *et al.*, 2007), the question whether maraviroc might increase frequency or severity of stroke needs to be addressed.

In summary, our results reveal a novel function of CCR5 in the CNS and suggest that the pharmacological interventions enhancing or decreasing CCR5 function could modify neuronal survival after ischaemia.

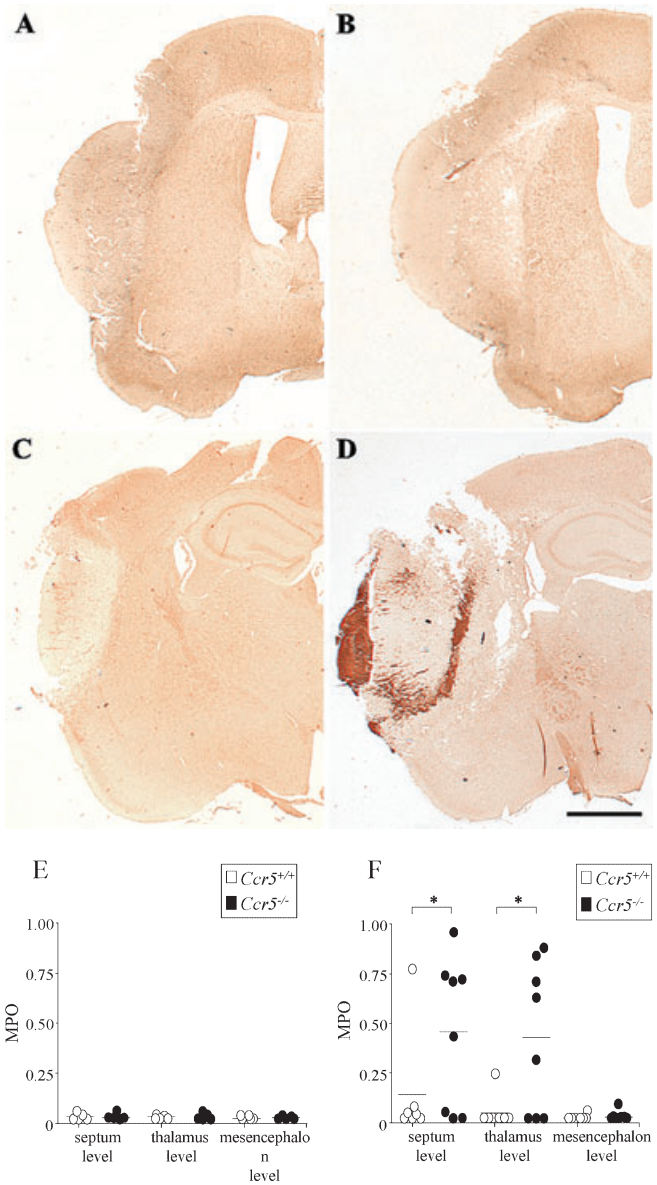

Figure 5 Neutrophil infiltration after middle cerebral artery occlusion (MCAo) in wild-type (*Ccr5*$^{+/+}$) and CCR5-deficient (*Ccr5*$^{-/-}$) mice. Neutrophils were detected by immunohistochemistry using an antibody against myeloperoxidase (MPO). (A–D) Representative brain sections of *Ccr5*$^{+/+}$ (A,C) and *Ccr5*$^{-/-}$ (B,D) mice stained with MPO antibody 2 days (A,B, $n = 5$) and 7 days (C,D, $n = 8$) after MCAo. Scale bar: 1 mm. (E,F) Quantification of the MPO staining in the infarct core 2 (E) and 7 (F) days after MCAo. The surface occupied by MPO-immunoreactive cells within the infarct core (*y*-axis) was quantified as described in the *Method* section. *$P < 0.05$ using Student's *t*-test ($n = 8$).

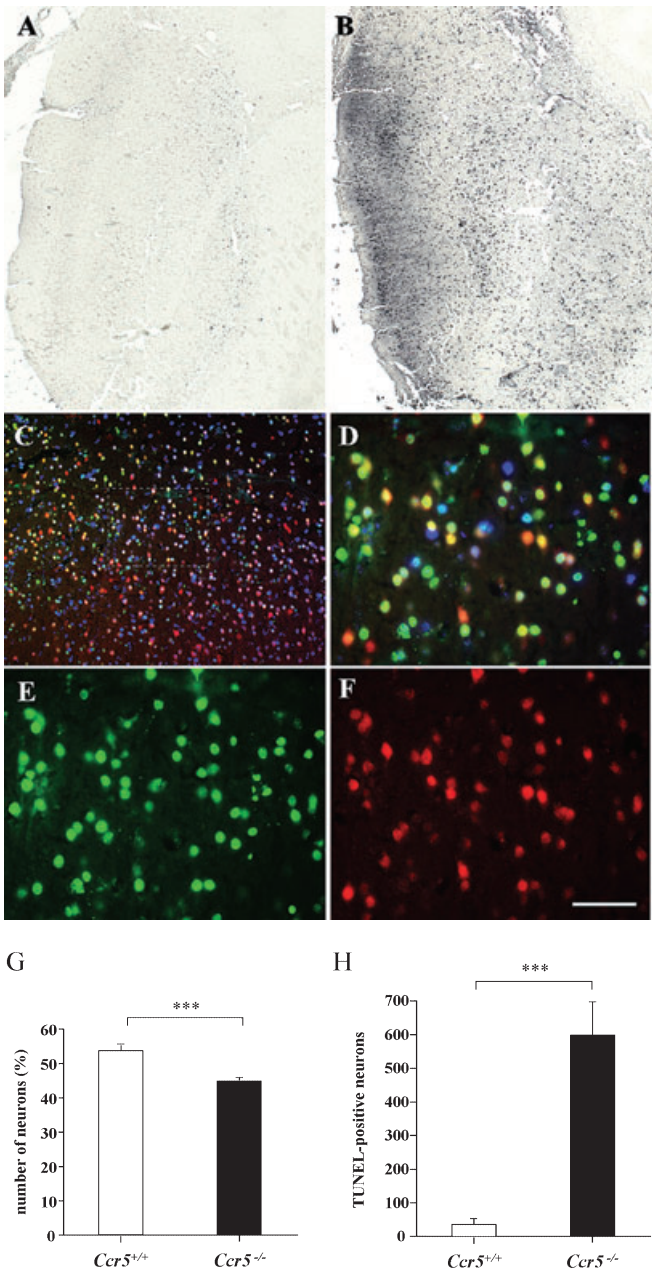

Figure 6 Increased neuronal death in CCR5-deficient (*Ccr5*$^{-/-}$) infarct brains. Neuronal death was analysed by immunohistochemistry on brain sections 7 days after middle cerebral artery occlusion. (A,B) Representative images of terminal deoxyribonucleotidyl transferase-mediated dUTP nick end labelling (TUNEL) staining in wild-type (*Ccr5*$^{+/+}$; A) and *Ccr5*$^{-/-}$ (B) ischaemic brains. (C–F) Representative image showing co-staining of TUNEL (green, E), NeuN (red, F) and DAPI (blue). Picture in (D) highlighted by dotted box in (C). Scale bars: (A,B) 340 μm; (C) 250 μm, (D–F) 80 μm. (G) Number of neurons in infarct regions normalized to the number of neurons in the corresponding contralateral parts. ***$P < 0.001$ *Ccr5*$^{+/+}$ versus *Ccr5*$^{-/-}$ using Student's *t*-test ($n = 6$). (H) Numbers of TUNEL-positive neurons in infarct regions. ***$P < 0.001$ using Student's *t*-test ($n = 6$).

Acknowledgements

The authors thank Dr Sergei Startchik from the Bioimaging Core Facility of the University of Geneva, Dr Oliver Hartley for advice and discussions and Dr C Edward Jefford for editing and comments. This work was supported by a grant from the Swiss National Foundation 3100A0-103725.

Conflicts of interest

The authors have no conflicting financial interests.

References

Afzal AR, Kiechl S, Daryani YP, Weerasinghe A, Zhang Y, Reindl M *et al*. (2008). Common CCR5-del32 frameshift mutation associated with serum levels of inflammatory markers and cardiovascular disease risk in the Bruneck population. *Stroke* **39**: 1972–1978.

Alexander SPH, Mathie A, Peters JA (2009). Guide to Receptors and Channels (GRAC), 4th edn. *Br J Pharmacol* **158**: S1–S254.

Alkhatib G, Combadiere C, Broder CC, Feng Y, Kennedy PE, Murphy PM *et al*. (1996). CC CKR5: a RANTES, MIP-1alpha, MIP-1beta receptor as a fusion cofactor for macrophage-tropic HIV-1. *Science* **272**: 1955–1958.

Babcock AA, Kuziel WA, Rivest S, Owens T (2003). Chemokine expression by glial cells directs leukocytes to sites of axonal injury in the CNS. *J Neurosci* **23**: 7922–7930.

Barr EL, Ouburg S, Igietseme JU, Morre SA, Okwandu E, Eko FO *et al*. (2005). Host inflammatory response and development of complications of Chlamydia trachomatis genital infection in CCR5-deficient mice and subfertile women with the CCR5delta32 gene deletion. *J Microbiol Immunol Infect* **38**: 244–254.

Beech JS, Reckless J, Mosedale DE, Grainger DJ, Williams SC, Menon DK (2001). Neuroprotection in ischemia-reperfusion injury: an anti-inflammatory approach using a novel broad-spectrum chemokine inhibitor. *J Cereb Blood Flow Metab* **21**: 683–689.

Blanpain C, Lee B, Tackoen M, Puffer B, Boom A, Libert F *et al*. (2000). Multiple nonfunctional alleles of CCR5 are frequent in various human populations. *Blood* **96**: 1638–1645.

Braunersreuther V, Zernecke A, Arnaud C, Liehn EA, Steffens S, Shagdarsuren E *et al*. (2007). Ccr5 but not Ccr1 deficiency reduces development of diet-induced atherosclerosis in mice. *Arterioscler Thromb Vasc Biol* **27**: 373–379.

Bruno V, Copani A, Besong G, Scoto G, Nicoletti F (2000). Neuroprotective activity of chemokines against N-methyl-D-aspartate or beta-amyloid-induced toxicity in culture. *Eur J Pharmacol* **399**: 117–121.

Cartier L, Hartley O, Dubois-Dauphin M, Krause KH (2005). Chemokine receptors in the central nervous system: role in brain inflammation and neurodegenerative diseases. *Brain Res Brain Res Rev* **48**: 16–42.

Catani MV, Corasaniti MT, Navarra M, Nistico G, Finazzi-Agro A, Melino G (2000). gp120 induces cell death in human neuroblastoma cells through the CXCR4 and CCR5 chemokine receptors. *J Neurochem* **74**: 2373–2379.

Cole JW, Pinto AN, Hebel JR, Buchholz DW, Earley CJ, Johnson CJ *et al*. (2004). Acquired immunodeficiency syndrome and the risk of stroke. *Stroke* **35**: 51–56.

Connolly ES, Jr, Winfree CJ, Stern DM, Solomon RA, Pinsky DJ (1996). Procedural and strain-related variables significantly affect outcome in a murine model of focal cerebral ischemia. *Neurosurgery* **38**: 523–531.discussion 532.

Cowell RM, Xu H, Galasso JM, Silverstein FS (2002). Hypoxic-ischemic injury induces macrophage inflammatory protein-1alpha expression in immature rat brain. *Stroke* **33**: 795–801.

Daberkow DP, Riedy MD, Kesner RP, Keefe KA (2007). Arc mRNA induction in striatal efferent neurons associated with response learning. *Eur J Neurosci* **26**: 228–241.

De Bilbao F, Guarin E, Nef P, Vallet P, Giannakopoulos P, Dubois-Dauphin M (2000). Cell death is prevented in thalamic fields but not in injured neocortical areas after permanent focal ischaemia in mice overexpressing the anti-apoptotic protein Bcl-2. *Eur J Neurosci* **12**: 921–934.

Dichgans M (2007). Genetics of ischaemic stroke. *Lancet Neurol* **6**: 149–161.

Dimitrijevic OB, Stamatovic SM, Keep RF, Andjelkovic AV (2007). Absence of the chemokine receptor CCR2 protects against cerebral ischemia/reperfusion injury in mice. *Stroke* **38**: 1345–1353.

Emmelkamp JM, Rockstroh JK (2007). CCR5 antagonists: comparison of efficacy, side-effects, pharmacokinetics and interactions – review of the literature. *Eur J Medical Res* **12**: 409–417.

Franklin KGB, Paxinos G (1997). *The Mouse Brain in Stereotaxic Coordinates*. Academic Press: San Diego, CA.

Galasso JM, Harrison JK, Silverstein FS (1998). Excitotoxic brain injury stimulates expression of the chemokine receptor CCR5 in neonatal rats. *Am J Pathol* **153**: 1631–1640.

Gamo K, Kiryu-Seo S, Konishi H, Aoki S, Matsushima K, Wada K *et al*. (2008). G-protein-coupled receptor screen reveals a role for chemokine receptor CCR5 in suppressing microglial neurotoxicity. *J Neurosci* **28**: 11980–11988.

Garau A, Bertini R, Colotta F, Casilli F, Bigini P, Cagnotto A *et al*. (2005). Neuroprotection with the CXCL8 inhibitor repertaxin in transient brain ischemia. *Cytokine* **30**: 125–131.

Garau A, Bertini R, Mosca M, Bizzarri C, Anacardio R, Triulzi S *et al*. (2006). Development of a systemically-active dual CXCR1/CXCR2 allosteric inhibitor and its efficacy in a model of transient cerebral ischemia in the rat. *Eur Cytokine Netw* **17**: 35–41.

Getts DR, Terry RL, Getts MT, Muller M, Rana S, Shrestha B *et al*. (2008). Ly6c+ 'inflammatory monocytes' are microglial precursors recruited in a pathogenic manner in West Nile virus encephalitis. *J Exp Medical* **205**: 2319–2337.

Glass WG, Lim JK, Cholera R, Pletnev AG, Gao JL, Murphy PM (2005). Chemokine receptor CCR5 promotes leukocyte trafficking to the brain and survival in West Nile virus infection. *J Exp Medical* **202**: 1087–1098.

Glass WG, McDermott DH, Lim JK, Lekhong S, Yu SF, Frank WA *et al*. (2006). CCR5 deficiency increases risk of symptomatic West Nile virus infection. *J Exp Medical* **203**: 35–40.

Haddad M, Rhinn H, Bloquel C, Coqueran B, Szabo C, Plotkine M *et al*. (2006). Anti-inflammatory effects of PJ34, a poly(ADP-ribose) polymerase inhibitor, in transient focal cerebral ischemia in mice. *Br J Pharmacol* **149**: 23–30.

Hardison JL, Wrightsman RA, Carpenter PM, Kuziel WA, Lane TE, Manning JE (2006). The CC chemokine receptor 5 is important in control of parasite replication and acute cardiac inflammation following infection with *Trypanosoma cruzi*. *Infect Immun* **74**: 135–143.

Huffnagle GB, McNeil LK, McDonald RA, Murphy JW, Toews GB, Maeda N *et al*. (1999). Cutting edge: role of C-C chemokine receptor 5 in organ-specific and innate immunity to *Cryptococcus neoformans*. *J Immunol* **163**: 4642–4646.

Hughes PM, Allegrini PR, Rudin M, Perry VH, Mir AK, Wiessner C (2002). Monocyte chemoattractant protein-1 deficiency is protective in a murine stroke model. *J Cereb Blood Flow Metab* **22**: 308–317.

Hunter AJ, Hatcher J, Virley D, Nelson P, Irving E, Hadingham SJ *et al*. (2000). Functional assessments in mice and rats after focal stroke. *Neuropharmacology* **39**: 806–816.

Kaul M, Lipton SA (1999). Chemokines and activated macrophages in HIV gp120-induced neuronal apoptosis. *Proc Natl Acad Sci USA* **96**: 8212–8216.

Kaul M, Lipton SA (2006). Mechanisms of neuroimmunity and neurodegeneration associated with HIV-1 infection and AIDS. *J Neuroimmune Pharmacol* **1**: 138–151.

Kaul M, Ma Q, Medders KE, Desai MK, Lipton SA (2007). HIV-1 coreceptors CCR5 and CXCR4 both mediate neuronal cell death but CCR5 paradoxically can also contribute to protection. *Cell Death Differ* **14**: 296–305.

Khan IA, Thomas SY, Moretto MM, Lee FS, Islam SA, Combe C *et al*. (2006). CCR5 is essential for NK cell trafficking and host survival following *Toxoplasma gondii* infection. *Plos Pathog* **2**.

Kremlev SG, Roberts RL, Palmer C (2007). Minocycline modulates chemokine receptors but not interleukin-10 mRNA expression in hypoxic-ischemic neonatal rat brain. *J Neurosci Res* **85**: 2450–2459.

Kuziel WA, Dawson TC, Quinones M, Garavito E, Chenaux G, Ahuja SS *et al*. (2003). CCR5 deficiency is not protective in the early stages of atherogenesis in apoE knockout mice. *Atherosclerosis* **167**: 25–32.

Libert F, Cochaux P, Beckman G, Samson M, Aksenova M, Cao A *et al*.

(1998). The deltaccr5 mutation conferring protection against HIV-1 in Caucasian populations has a single and recent origin in Northeastern Europe. *Hum Mol Genet* **7**: 399–406.

Lim JK, Louie CY, Glaser C, Jean C, Johnson B, Johnson H *et al*. (2008). Genetic deficiency of chemokine receptor CCR5 is a strong risk factor for symptomatic West Nile virus infection: a meta-analysis of 4 cohorts in the US epidemic. *J Infect Dis* **197**: 262–265.

Liu R, Paxton WA, Choe S, Ceradini D, Martin SR, Horuk R *et al*. (1996). Homozygous defect in HIV-1 coreceptor accounts for resistance of some multiply-exposed individuals to HIV-1 infection. *Cell* **86**: 367–377.

Ma B, Kang MJ, Lee CG, Chapoval S, Liu W, Chen Q *et al*. (2005). Role of CCR5 in IFN-gamma-induced and cigarette smoke-induced emphysema. *J Clin Invest* **115**: 3460–3472.

Maeda K, Hata R, Hossmann KA (1998). Differences in the cerebrovascular anatomy of C57black/6 and SV129 mice. *Neuroreport* **9**: 1317–1319.

Mallolas J, Hurtado O, Castellanos M, Blanco M, Sobrino T, Serena J *et al*. (2006). A polymorphism in the EAAT2 promoter is associated with higher glutamate concentrations and higher frequency of progressing stroke. *J Exp Medical* **203**: 711–717.

Martinson JJ, Chapman NH, Rees DC, Liu YT, Clegg JB (1997). Global distribution of the CCR5 gene 32-basepair deletion. *Nat Genet* **16**: 100–103.

Mehta SL, Manhas N, Raghubir R (2007). Molecular targets in cerebral ischemia for developing novel therapeutics. *Brain Res Rev* **54**: 34–66.

Meucci O, Fatatis A, Simen AA, Bushell TJ, Gray PW, Miller RJ (1998). Chemokines regulate hippocampal neuronal signaling and gp120 neurotoxicity. *Proc Natl Acad Sci USA* **95**: 14500–14505.

Oppermann M (2004). Chemokine receptor CCR5: insights into structure, function, and regulation. *Cell Signal* **16**: 1201–1210.

Roppolo D, Vollery S, Kan CD, Luscher C, Broillet MC, Rodriguez I (2007). Gene cluster lock after pheromone receptor gene choice. *EMBO J* **26**: 3423–3430.

Rossi D, Zlotnik A (2000). The biology of chemokines and their receptors. *Annu Rev Immunol* **18**: 217–242.

Rostene W, Kitabgi P, Parsadaniantz SM (2007). Chemokines: a new class of neuromodulator? *Nat Rev Neurosci* **8**: 895–903.

Rottman JB, Ganley KP, Williams K, Wu L, Mackay CR, Ringler DJ (1997). Cellular localization of the chemokine receptor CCR5. Correlation to cellular targets of HIV-1 infection. *Am J Pathol* **151**: 1341–1351.

Saita Y, Kondo M, Shimizu Y (2007). Species selectivity of small-molecular antagonists for the CCR5 chemokine receptor. *Int Immunopharmacol* **7**: 1528–1534.

Sayana S, Khanlou H (2009). Maraviroc: a new CCR5 antagonist. *Expert Rev Anti Infect Ther* **7**: 9–19.

Schroeter M, Zickler P, Denhardt DT, Hartung HP, Jander S (2006). Increased thalamic neurodegeneration following ischaemic cortical stroke in osteopontin-deficient mice. *Brain* **129**: 1426–1437.

Simpson J, Rezaie P, Newcombe J, Cuzner ML, Male D, Woodroofe MN (2000). Expression of the beta-chemokine receptors CCR2, CCR3 and CCR5 in multiple sclerosis central nervous system tissue. *J Neuroimmunol* **108**: 192–200.

Sonomura T, Nakamura K, Furuta T, Hioki H, Nishi A, Yamanaka A *et al*. (2007). Expression of D1 but not D2 dopamine receptors in striatal neurons producing neurokinin B in rats. *Eur J Neurosci* **26**: 3093–3103.

Soriano SG, Amaravadi LS, Wang YF, Zhou H, Yu GX, Tonra JR *et al*. (2002). Mice deficient in fractalkine are less susceptible to cerebral ischemia-reperfusion injury. *J Neuroimmunol* **125**: 59–65.

Spleiss O, Gourmala N, Boddeke HW, Sauter A, Fiebich BL, Berger M *et al*. (1998). Cloning of rat HIV-1-chemokine coreceptor CKR5 from microglia and up-regulation of its mRNA in ischemic and endotoxinemic rat brain. *J Neurosci Res* **53**: 16–28.

Stephenson J (2007). Researchers buoyed by novel HIV drugs: will expand drug arsenal against resistant virus. *JAMA* **297**: 1535–1536.

Takami S, Minami M, Nagata I, Namura S, Satoh M (2001). Chemokine receptor antagonist peptide, viral MIP-II, protects the brain against focal cerebral ischemia in mice. *J Cereb Blood Flow Metab* **21**: 1430–1435.

Takami S, Minami M, Katayama T, Nagata I, Namura S, Satoh M (2002). TAK-779, a nonpeptide CC chemokine receptor antagonist, protects the brain against focal cerebral ischemia in mice. *J Cereb Blood Flow Metab* **22**: 780–784.

Thapa M, Kuziel WA, Carr DJ (2007). Susceptibility of CCR5-deficient mice to genital herpes simplex virus type 2 is linked to NK cell mobilization. *J Virol* **81**: 3704–3713.

Tipping B, de Villiers L, Wainwright H, Candy S, Bryer A (2007). Stroke in patients with human immunodeficiency virus infection. *J Neurol Neurosurg Psychiatry* **78**: 1320–1324.

Torres-Munoz JE, Van Waveren C, Keegan MG, Bookman RJ, Petito CK (2004). Gene expression profiles in microdissected neurons from human hippocampal subregions. *Brain Res Mol Brain Res* **127**: 105–114.

Wang Q, Tang XN, Yenari MA (2007). The inflammatory response in stroke. *J Neuroimmunol* **184**: 53–68.

Westmoreland SV, Alvarez X, deBakker C, Aye P, Wilson ML, Williams KC *et al*. (2002). Developmental expression patterns of CCR5 and CXCR4 in the rhesus macaque brain. *J Neuroimmunol* **122**: 146–158.

Zausinger S, Hungerhuber E, Baethmann A, Reulen H, Schmid-Elsaesser R (2000). Neurological impairment in rats after transient middle cerebral artery occlusion: a comparative study under various treatment paradigms. *Brain Res* **863**: 94–105.

Supporting information

Additional Supporting Information may be found in the online version of this article:

Video S1 Representative videos of *Ccr5*$^{+/+}$ and *Ccr5*$^{-/-}$ mice during the grip test. (Video01) *Ccr5*$^{+/+}$ and (Video02) *Ccr5*$^{-/-}$ mice 24 h after permanent middle cerebral artery occlusion.

Please note: Wiley-Blackwell are not responsible for the content or functionality of any supporting materials supplied by the authors. Any queries (other than missing material) should be directed to the corresponding author for the article.